Surface Science Letters 274 (1992) L611–L618
North-Holland

surface science
letters

Surface Science Letters

CO adsorption on Pd(111): the effects of temperature and pressure

W. Kevin Kuhn, János Szanyi and D. Wayne Goodman
Department of Chemistry, Texas A&M University, College Station, TX 77843, USA

Received 8 April 1992; accepted for publication 8 May 1992

Infrared reflection-absorption spectroscopy (IRAS) has been used to study the adsorption of carbon monoxide on a Pd(111) surface. IRAS spectra were collected at temperatures from 100 to 1000 K and at pressures from 1.0×10^{-7} to 10.0 Torr. The IRAS data at temperatures > 250 K showed the coverage versus temperature behavior anticipated from the data acquired under UHV conditions. However, at temperatures < 250 K, multiple CO adsorption structures were observed which were dependent upon the adsorption temperature and pressure. The low temperature/low pressure adsorption data extrapolate to the high temperature/high pressure regime only if appropriate adsorption conditions are employed.

1. Introduction

The use of single-crystal metal surfaces as models of "real-world" catalysts has provided valuable information regarding reaction mechanisms. However, these data are generally acquired under ultrahigh vacuum (UHV) and low temperature conditions, whereas typical catalytic processes operate at high temperatures (e.g. > 300 K) and pressures above one atmosphere. Because of this disparity some have questioned the relevance of the UHV studies to "real world" catalytic processes. During recent years, work has been carried out to bridge this "pressure gap" by combining a UHV chamber with a high pressure catalytic reactor [1]. In these studies, the reactions are run at temperatures and pressures which are comparable to the conditions used in typical catalytic processes. However, an ex situ analysis of the sample is generally employed because of the UHV requirements of the usual surface spectroscopic techniques. Recently, studies have bridged the "pressure gap" in a more direct fashion by studying adsorption in situ at elevated pressures and temperatures using infrared reflection-absorption spectroscopy (IRAS) [2–6]. For example, high pressure studies of CO adsorption on Cu(100) have indicated that the results obtained at UHV pressures and temperatures < 200 K extrapolate remarkable well into the high pressure/high temperature regime [6].

Previous studies of the CO/Pd(111) system using IRAS [7,8] and temperature programmed desorption (TPD) [9,10] have shown that there are multiple CO adsorption sites and structures. In addition, it has been shown that despite the smoothness of the Pd(111) surface, CO adsorption at 90 K yields a quite different desorption energy (E_d) versus coverage relationship than that obtained for CO adsorption at 200 K [10].

To gain further insight into the correspondence (or lack thereof) between UHV and high pressure adsorption data, we report the results of a study of CO adsorption on Pd(111) over a wide range of pressures and temperatures (100–1000 K and 1×10^{-7}–10.0 Torr). This study shows that within certain constraints, UHV/low temperature studies can be used to accurately model the high pressure/high temperature adsorption regime for the CO/Pd(111) system.

2. Experimental

The experiments were performed in an UHV chamber (base pressure $\leq 5 \times 10^{-10}$ Torr) equipped for IRAS, Auger electron spectroscopy (AES), low-energy electron diffraction (LEED) and TPD. This apparatus has been described in detail elsewhere [11,12]. The IR cell has CaF_2 windows and is interfaced to the UHV chamber via a sliding seal which allows experiments to be conducted at pressures as high as several atmospheres. In this work the CO pressure in the IR cell was varied from 1×10^{-8} to 10 Torr. Pressures from 1×10^{-9}–1×10^{-3} Torr were measured using a nude ionization gauge, while pressures from 0.01–10.00 Torr were monitored using a 10 Torr Baratron gauge.

The IRAS spectra were acquired for 512 scans in the single reflection mode at a resolution of 8 cm^{-1} and an incidence angle of 85° from the surface normal. In order to eliminate the contribution of gas-phase CO to the absorption spectra (which becomes noticeable for $P_{CO} > 10^{-3}$ Torr) background spectra were collected at temperatures sufficiently high that no appreciable CO remained adsorbed. In other words, for CO pressures from 10^{-7} to 10 Torr, the corresponding background IRAS spectra were acquired at temperatures from 650 to 1000 K. At these temperatures, the amount of CO adsorbed on the surface is negligible and thus the background spectrum will only contain features due to gas-phase CO. Thus, at elevated pressures, the IRAS features due to adsorbed CO are found by subtracting the corresponding background spectrum from the spectrum acquired at the temperature of interest [6].

The manipulator allowed resistive heating to 1500 K and liquid nitrogen cooling to 90 K with the sample temperature being monitored by a W–5%Re/W–26%Re thermocouple. Carbon monoxide (99.995% from Matheson Gas Products) was stored in a glass bulb at liquid nitrogen temperature throughout the study to preclude metal carbonyl contamination of the CO admitted into the IR cell. The surface was cleaned using the procedures in ref. [13] followed by annealing at 1200 K. The cleanliness and long-range order of the surface were verified with AES and LEED, respectively.

3. Results and discussion

In fig. 1, a series of IR spectra acquired at a CO pressure of 10.0 Torr is displayed as a function of sample temperature. These spectra show CO adsorption progressing from three-fold hollow sites, to bridging sites, and then to a combination of a-top and three-fold hollow sites as the sample temperature is lowered. This bonding site progression has been observed previously in isothermal coverage dependent UHV studies of the IR spectra of CO adsorbed on Pd(111) [7,8]. The peak frequencies observed in these earlier studies [7,8] were used as the basis for the bond-

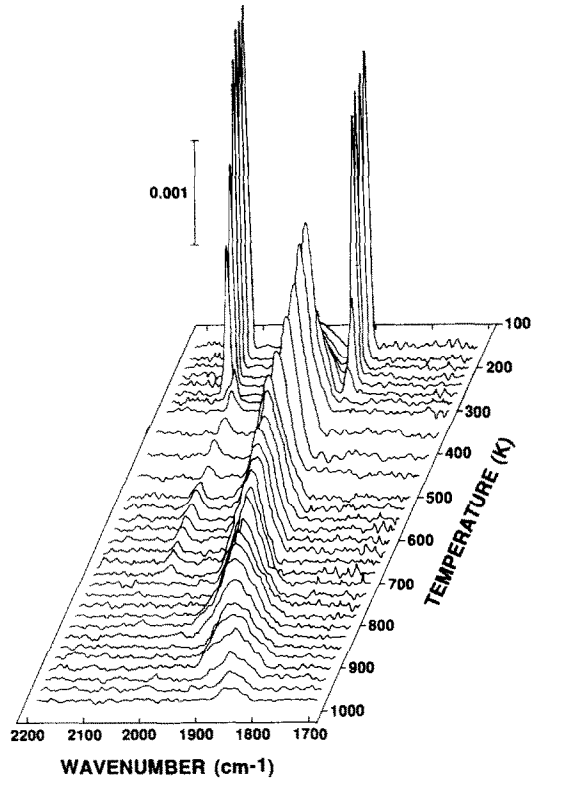

Fig. 1. IR spectra of CO on Pd(111) at $P_{CO} = 10.0$ Torr as a function of temperature. The spectra were collected from high temperature to low temperature.

ing site assignments used in this study. In addition, this bonding site progression has been corroborated by changes in the adsorption energy of CO [14] as well as changes in the observed LEED patterns [15] as the CO coverage is increased. In addition, a study of CO adsorption on ~ 75 Å Pd crystals on SiO_2 has shown that a CO coverage increase at 80 K will cause a reduction in bridging CO with a concomitant increase in a-top and three-fold hollow CO [16]. The peak frequencies for the a-top and hollow features from the supported Pd sample were 2103 and 1883 cm^{-1}, respectively, remarkably close to the 2110 and 1895 cm^{-1} values observed in this work. However, for the supported Pd, even at maximum coverage (108 Torr at 80 K) a feature at ~ 1995 cm^{-1} attributable to bridging CO remained [16]. The observed differences between the supported Pd and single crystal Pd are likely attributable to a reduction in the magnitude of the lateral interactions between the adsorbed CO's on the 75 Å supported Pd crystallites or to the presence of additional crystal facets (e.g. (100) or (110)) which could give rise to features not seen for Pd(111). For the 10 Torr data shown in fig. 1, the transition from hollow to bridging adsorption occurred at ~ 850–900 K and the transition from bridging to a-top/hollow occurred at ~ 250 K. Although the hollow to bridging transition is not sharp in fig. 1, previous UHV studies [7,8], as well as other data in this study (see for example, fig. 2), have shown that there is indeed a transition from one bonding site to the other as deduced from the IR peak position change from ~ 1855 to ~ 1900 cm^{-1}. These peak position changes are not due to temperature changes but must arise from changes in CO coverage since the peak shifts observed in this study agree quite well with the shifts observed in previous coverage dependent isothermal studies [7,8]. In the high temperature/low coverage limit, the peak corresponding to CO adsorbed in a three-fold hollow typically appeared at ~ 1825 cm^{-1}. The peak corresponding to bridge-bound CO was at ~ 1950 cm^{-1} and the combination a-top/three-fold hollow configuration gave rise to peaks at 2105 and 1895 cm^{-1}, respectively. In addition to these intense CO stretching features, there is a weak feature at

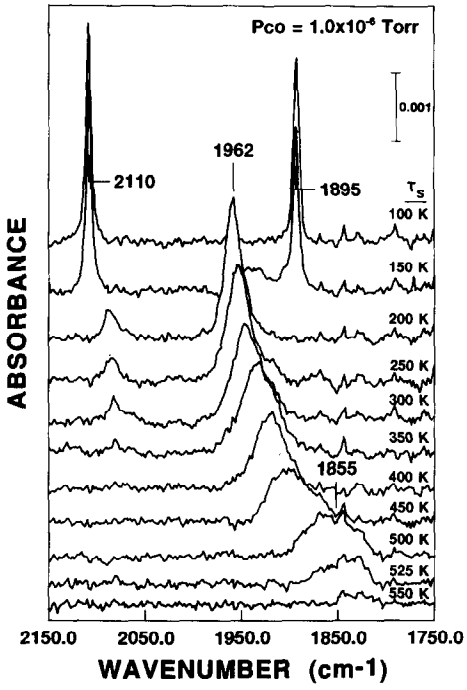

Fig. 2. IR spectra of CO on Pd(111) at $P_{CO} = 1.0 \times 10^{-6}$ Torr as a function of temperature. The spectra were collected from high temperature to low temperature.

2096 cm^{-1} that appears at 720 K and persists until the bridging → a-top/hollow phase transition occurs at ~ 250 K. This peak is likely due to small amounts of CO adsorbed on top of Pd atoms and could represent either a slight disorder on the CO overlayer or a mismatch between the compressed CO(4 × 2) overlayer and the Pd(111) substrate that forces some CO onto a-top sites.

In addition to the 10.0 Torr data shown in fig. 1, isobaric adsorption data have been collected at every decade from 10^{-7} to 10.0 Torr. In each of these isobaric series, the adsorption site progression is identical. The only apparent differences are the temperatures at which the adsorption site transformations occur. (For example, compare the 10.0 Torr data shown in fig. 1 with the 1.0×10^{-6} Torr data shown in fig. 2.) As the CO pressure is increased from 10^{-7} to 10.0 Torr, the IR spectra show that the temperature at which the CO coverage approaches zero increases from ~ 550 to ~ 1000 K. The low pressure results are in agree-

ment with TPD data which show that CO desorption occurs at ~ 500 K in UHV [9,10]. Isosteric plots, obtained from the isobaric data discussed elsewhere [17], indicate a desorption activation energy of ~ 30 kcal/mol (in agreement with previous observations [10,15]).

LEED results from the various CO bonding configurations are shown in fig. 3 and are in

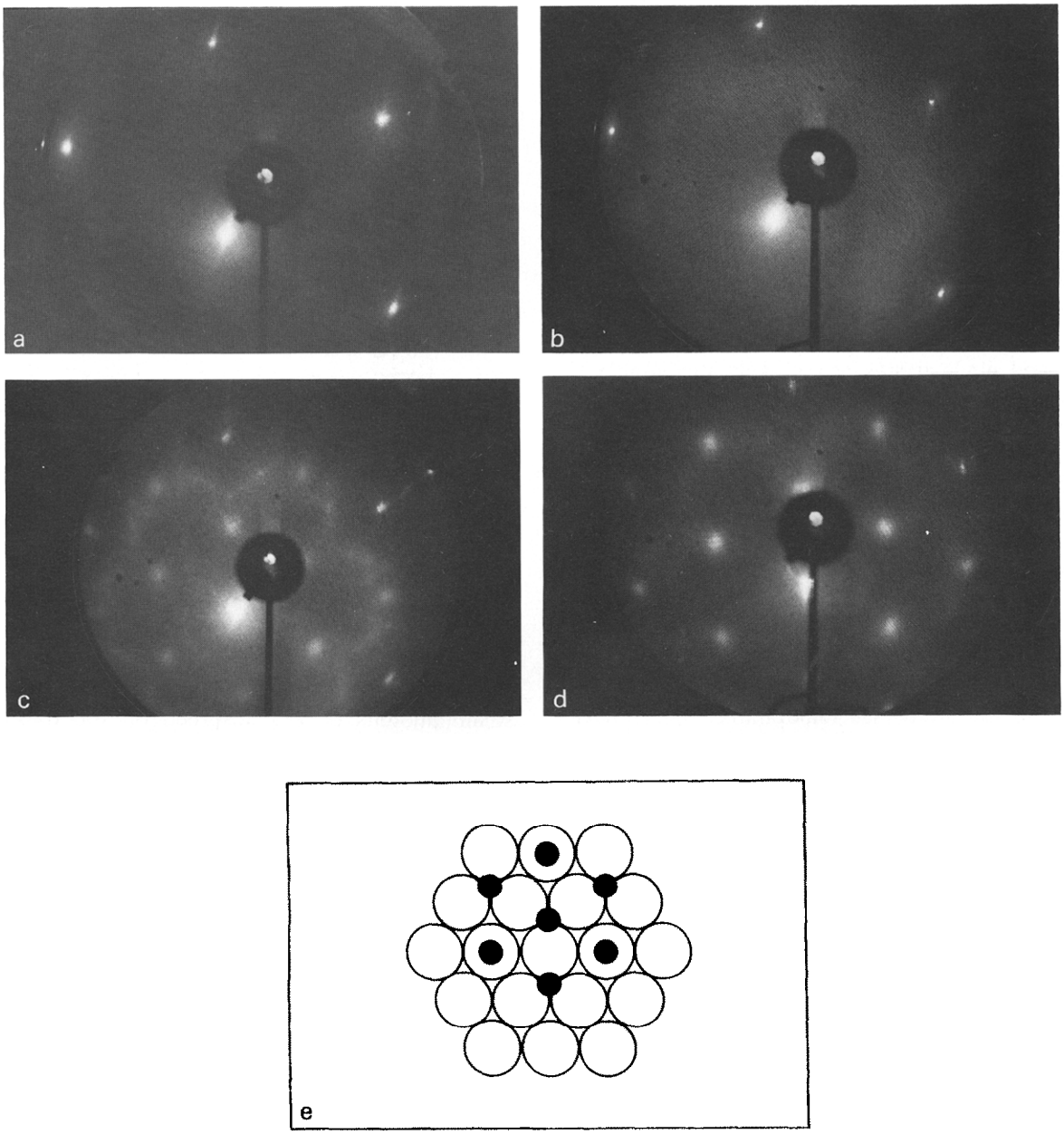

Fig. 3. LEED patterns for different CO structures on Pd(111). (a) Clean substrate (97 eV); (b) saturation CO at 90 K (96 eV); (c) at 90 K after annealing to 150 K in 1×10^{-6} Torr CO, "split" (2×2) pattern (91 eV); (d) at 90 K after annealing to 600 K in 1×10^{-6} Torr CO, (2×2) pattern (88 eV); (e) a real space structure model of the (2×2) structure.

complete agreement with previous work [7,8,15]. The sharp (2 × 2) LEED structure in fig. 3d corresponds to the 100 K IRAS spectra that exhibit sharp features due to a-top/hollow CO adsorption. Thus both LEED and IRAS indicate a highly ordered CO phase. In previous studies, this phase was typically characterized by a diffuse (2 × 2) LEED pattern and additional IR peaks [8,15]. The sharp (2 × 2) LEED pattern and sharp a-top/hollow IR features are in excellent agreement with the proposed CO structure at this coverage [8] as shown in fig. 3e.

Fig. 4 clearly shows that the IRAS spectra are strongly dependent upon the sample preparation conditions. All IR spectra in this figure were acquired at 90 K with $P_{CO} = 1.0 \times 10^{-6}$ Torr. The only difference between spectra a, b, c, and d is the temperature to which the sample was annealed (in the presence of 1×10^{-6} Torr CO) prior to cooling (90 K) for spectral acquisition. For fig. 4a, the sample remained unannealed at 90 K, while for b, c, and d the sample was annealed to 200, 400, and 600 K in 1×10^{-6} Torr CO, respectively, then cooled to 90 K for IR spectral acquisition. After the IR spectrum was collected, the CO was pumped out, the sample returned to the UHV chamber and the corresponding TPD spectrum acquired. It should be noted that returning the sample to UHV conditions at 90 K had no measurable effect on the adsorbed CO. At this temperature, the IR spectra acquired after the gas-phase CO was removed were essentially identical to those obtained in the presence of CO. The TPD data for a saturation CO exposure at 90 K following an anneal to 200 K agrees with previous TPD results [9,10]. The main desorption feature is at ~500 K with a broad desorption band extending down to ~200–300 K.

The marked differences in the CO IR spectra in fig. 4 can be understood by comparing the IRAS and TPD data shown in fig. 4 to the equilibrium IRAS data shown in fig. 2. Fig. 2 shows that for $P_{CO} = 1.0 \times 10^{-6}$ Torr the three structural transitions (a-top/hollow → bridging, bridging → three-fold hollow, and hollow → gas phase) occur at ~170, ~470, and ~560 K, respectively. The three annealing temperatures used for the data shown in fig. 4, thus, result in increasingly lower CO coverages corresponding

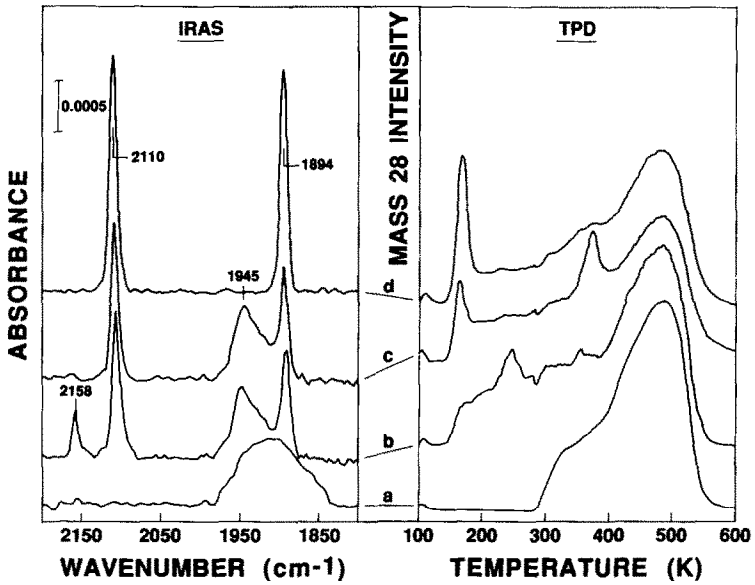

Fig. 4. Correlation between IRAS and TPD spectra of CO/Pd(111) as a function of anneal temperature with $P_{CO} = 1 \times 10^{-6}$ Torr. All IR spectra were acquired at 90 K. Anneal temperatures were 90 K (a), 200 K (b), 400 K (c), and 600 K (d).

to the coverage–temperature equilibrium at 1.0×10^{-6} Torr. As the sample is cooled to 90 K (still in the presence of 1.0×10^{-6} Torr CO), the CO coverage increases to form a more highly ordered CO structure. The changes observed in fig. 4, therefore, are due to increased CO adsorption during the temperature quench leading to a more densely packed, more highly ordered overlayer, and not simply to a thermally induced restructuring of the initial CO overlayer. Integration of the CO TPD features for the unannealed and fully ordered surfaces showed that there is some redistribution of intensity from the 500 K peak to lower temperatures. However, the total intensity of the ordered surface is 10–20% higher than for the unannealed surface confirming the increase in CO coverage. In addition, a sample exposed to 1.0×10^{-6} Torr CO at 90 K, annealed in vacuo to 200 K, then cooled to 90 K for spectral collection, shows only CO adsorbed on bridging sites. That is, there was no reordering of the CO into the predominantly a-top/hollow configuration as seen in fig. 4b. Apparently, the CO coverage following a saturation exposure at 90 K is insufficient to facilitate the phase transition between the bridging and a-top/hollow configurations.

TPD after annealing to 600 K and cooling back to 90 K in 1×10^{-6} Torr CO clearly shows a loss of CO occurring at ~ 170 K due to the transition from a-top/hollow to bridging adsorption sites. The sharp desorption feature at 370 K for the 400 K anneal in fig. 4c is likely related to the presence of excess bridging CO on a surface that has a predominantly a-top/hollow configuration. Repeated annealing/cooling cycles to ~ 150 K (lower than necessary for the phase equilibration) yielded IR spectra with a prominent feature at ~ 1950 cm^{-1} and smaller features at 2110 and 1893 cm^{-1}. A TPD from this surface typically showed a prominent desorption feature at ~ 370 K ($2 \times$ the 500 K peak intensity) and a smaller feature at 500 K. The 370 K peak is tentatively assigned to correspond to the desorption of CO arising from the loss of bridge-bound CO. This suggests that for this adsorption configuration, domains of bridge-bound CO do not transform into hollow sites during the thermal

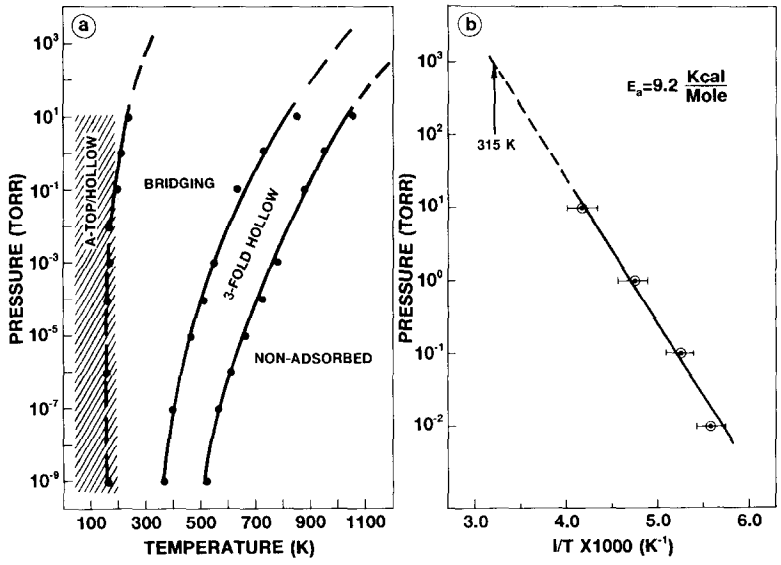

Fig. 5. (a) CO/Pd(111) equilibrium pressure–temperature phase diagram showing the different CO adsorption phases: a-top/three-fold hollow, bridging, three-fold hollow, and non-adsorbed. (b) An isosteric plot of the transition from a-top/three-fold hollow to bridging CO.

desorption process and, therefore, do not contribute to the desorption peak at ~ 500 K. Although much caution must be exercised in the correlation between adsorption phases and TPD features, the results shown in fig. 4 suggest that CO desorption from Pd(111) proceeds as a reversal of the structural changes which occur during adsorption. If this were the case, the TPD peaks at ~ 170, ~ 370, and ~ 500 K then correspond to CO desorption due to transitions from a-top/hollow → bridging, bridging → hollow, and hollow → desorbed CO. Data obtained at 1×10^{-6} Torr indicate that this is indeed the case. As the temperature is increased from 100–600 K, CO bonding changes from a-top/hollow → bridging → hollow → desorbed.

An intriguing feature in fig. 4b is the peak at 2158 cm^{-1} since this peak is at a frequency that is higher than gas-phase CO (2143 cm^{-1}). A peak at 2159 cm^{-1} was observed in a previous study of Pd supported on SiO_2 at 80 K and CO pressures ≥ 100 mTorr, and was attributed to CO physisorbed on the SiO_2 support [16]. The origin of the 2158 cm^{-1} peak in this work is not clear, however, it likely relates to surface defects (e.g. step edges) that are only populated when the disordered CO layer shown in fig. 4a is heated to 150–250 K. The apparent intensity of this peak is probably significantly enhanced due to intensity sharing from the 2110 cm^{-1} peak [18]. Thus, the actual surface concentration of the species giving rise to this feature is likely much lower than its intensity might suggest.

As mentioned above, adsorption data have been collected over temperatures ranging from 90 to 1000 K and pressures ranging from 10^{-7} to 10.0 Torr. This allows the construction of the equilibrium phase diagram shown in fig. 5a. It should be noted, however, especially for the transition from bridging to a-top/hollow adsorption, that these transitions are for the fully equilibrated system. It is possible, especially at low temperatures, for a non-equilibrium CO adsorption configuration to occur. This is exemplified by spectra a, b and c in fig. 4. It has been found that non-equilibrium adsorption can occur at temperatures < 200 K as indicated by the cross-hatched region in fig. 5a. In this region a variety of non-equilibrium adsorption configurations is possible and the true equilibrium adsorption structure is only obtainable if the appropriate adsorption conditions are used, as has been discussed above. It is clear from fig. 5, however, that the equilibrium adsorption structures obtained at low pressures and temperatures are contiguous with the high pressure/high temperature structures.

Fig. 5b shows the pressure–temperature dependence of the transition from bridging to a-top/hollow site adsorption plotted in the form of an isosteric plot. This assumes that the onset of this transition corresponds to a critical coverage of CO. Extrapolation to a CO pressure of 1000 Torr yields a transition temperature of ~ 315 K. This suggests that at ambient temperatures, a CO pressure of ~ 1000 Torr would give rise to a-top/hollow CO as the stable adsorption site configuration. These data also allow the calculation of an adsorption energy for the CO giving rise to the phase transition. The 9.2 ± 1.8 kcal/mol value obtained is in good agreement with the 9.5 kcal/mol desorption energy calculated from the 170 K desorption peak in the TPD spectra of fig. 4 applying the Redhead approximation and assuming $\nu = 10^{13}$.

4. Summary and conclusions

This study of CO adsorption on Pd(111) has shown that the IR spectra of adsorbed CO are strongly dependent on sample preparation conditions. This does not preclude, however, the use of low temperature UHV studies to model the behavior of CO on Pd(111) at elevated pressure–temperature conditions. An equilibrium phase diagram has been constructed showing the continuity of the CO adsorption phases as pressure and temperature are increased. Therefore, under the appropriate conditions, UHV studies for the CO/Pd(111) system can be used to model the elevated pressure regime. However, additional studies are required to determine if true equilibrium adsorption structures are accessible under UHV conditions for other strongly bound CO–metal systems.

Acknowledgement

We acknowledge with pleasure the support of this work by the Department of Energy, Office of Basic Energy Sciences, Division of Chemical Science.

References

[1] J.A. Rodriguez and D.W. Goodman, Surf. Sci. Rep. 14 (1991) 1, and references therein.
[2] (a) R. Burch, Ed., In Situ Methods in Catalysis, Catal. Today, Vol. 9 (Elsevier, Amsterdam, 1991);
(b) D.J. Dwyer and F.M. Hoffmann, Eds., Surface Science of Catalysis, In Situ Probes and Reaction Kinetics, ACS Symposium Series 482 (American Chemical Society, Washington DC, 1992).
[3] V.A. Burrows, S. Sundarensan, Y.J. Chabal and S.B. Christmann, Surf. Sci. 180 (1987) 110.
[4] A.S. Glass and V.M. Bermudez, J. Vac. Sci. Technol. A 8 (1990) 2622.
[5] (a) F.M. Hoffmann and J.L. Robbins, J. Vac. Sci. Technol. A 5 (1987) 724;
(b) C.H.F. Peden, D.W. Goodman, M.D. Weisel and F.M. Hoffmann, Surf. Sci. 253 (1991) 44.
[6] C.M. Truong, J.A. Rodriguez and D.W. Goodman, Surf. Sci. Lett. 271 (1992) L385.
[7] A.M. Bradshaw and F.M. Hoffmann, Surf. Sci. 72 (1978) 513.
[8] F.M. Hoffmann, Surf. Sci. Rep. 3 (1983) 103.
[9] M.P. Kiskinova and G.M. Bliznakov, Surf. Sci. 123 (1982) 61.
[10] X. Guo and J.T. Yates, Jr., J. Chem. Phys. 90 (1989) 6761.
[11] L.-W.H. Leung, J.-W. He and D.W. Goodman, J. Chem. Phys. 93 (1990) 8378.
[12] R.A. Campbell and D.W. Goodman, Rev. Sci. Instrum. 63 (1992) 172.
[13] M. Grunze, H. Ruppender and O. Elshazly, J. Vac. Sci. Technol. A 6 (1988) 1266.
[14] (a) G. Ertl and J. Koch, in: Adsorption–Desorption Phenomena, Ed. F. Ricca (Academic Press, New York, 1972) p. 345;
(b) H. Conrad, G. Ertl, J. Koch and E.E. Latta, Surf. Sci. 43 (1974) 462.
[15] H. Conrad, G. Ertl and J. Küppers, Surf. Sci. 76 (1978) 323.
[16] (a) P. Gelin and J.T. Yates, Jr., Surf. Sci. 136 (1984) L1;
(b) P. Gelin, A.R. Siedle and J.T. Yates, Jr., J. Phys. Chem. 88 (1984) 2978.
[17] W.K. Kuhn, J. Szanyi and D.W. Goodman, in preparation.
[18] (a) R. Ryberg, Adv. Chem. Phys. 76 (1989) 1;
(b) V.M. Browne, S.G. Fox and P. Hollins, Catal. Today 9 (1991) 1;
(c) J.A. Rodriguez, C.M. Truong and D.W. Goodman, Surf. Sci. Lett. 271 (1992) L331.